Influence of oxygen octahedron distortion on the e_g states in manganites: Isotope effect

S. W. Biernacki*
Institute of Physics, Polish Academy of Sciences, Al. Lotnikow 32/46, 02-668 Warsaw, Poland
(Received 13 December 2001; published 6 September 2002)

A model of the spontaneous ferromagnetic ordering in the $La_{1-x}Ca_xMnO_3$ ($x \approx 0.2$–0.33) crystals is described. The partition function of the ferromagnetic to paramagnetic phase transition is determined, and the Curie temperature T_C is expressed in terms of the two parameters. The parameters describe the binding energy of the e_g electrons between two neighboring Mn ions and the Jahn-Teller energy of e_g electron. Since at a temperature close to T_C the partition function undergoes an abrupt drop, the crystal exhibits unusual changes in its properties at this temperature. The change of the specific-heat capacity, C_V, is calculated. The isotope shift of the critical temperature upon substitution of ^{16}O by ^{18}O is also calculated. The influence of the magnetic field on the resistivity is discussed.

DOI: 10.1103/PhysRevB.66.094405 PACS number(s): 75.40.Cx, 64.60.Cn, 75.10.Hk, 75.50.Dd

I. INTRODUCTION

The perovskites, such as $La_{1-x}Ca_xMnO_3$, exhibit unusual magnetic properties. The system with a nominal doping of $0.2 \leqslant x \leqslant 0.5$ undergoes a ferromagnetic to paramagnetic (FP) phase transition at the Curie temperature, T_C. Since the FP transition is accompanied by a large increase in resistance, it is also referred to as a metal-to-insulator transition. The basis for a theoretical understanding of the $La_{1-x}Ca_xMnO_3$ perovskites is usually the double-exchange mechanism introduced by Zener.[1] Recently, the double-exchange mechanism, which is the basis for a description of the physics of colossal magnetoresistance (CMR) in manganites, was reviewed by Izymov and Skryabin.[2] In particular, they discussed the application of the dynamical mean-field method to double-exchange systems.[3] On the other hand, Zhao[4] suggested that the double exchange mechanism is not the primary source of the ferromagnetism in doped manganites. The double-exchange itself ignores the effect of lattice motion on magnetic properties. The recent observation[5–8] of the isotope shift of the critical temperature T_C in the lanthanum manganites demonstrates the importance of the electron-lattice interaction. The electron-phonon interaction has been proposed to explain a giant oxygen-isotope shift, an anomalous volume change near T_C (Refs. 9 and 10), and the strong pressure dependence of some physical properties.[11,12] Specific-heat measurements[13–16] have revealed that the $La_{1-x}Ca_xMnO_3$ crystals with doping $x \approx 0.2$–0.33 exhibit a sharp specific heat peak associated with the FP transition. The large entropy change at the critical temperature T_C was also reported in Refs. 13 and 16.

These observations point to the importance of the Jahn-Teller (JT) distortion on the phase transition. Here we describe a phenomenological statistical model which accounts not only for the purely electronic degrees of freedom but also takes into account the electron-phonon coupling. The model contains two adjustable parameters; it reproduces the abrupt drop of the spin ordering at T_C and, consequently, the sharp peak of the specific-heat capacity. The large isotope shift of the phase transition temperature is calculated without employing additional parameters. The CMR is also discussed.

II. MODEL OF PHASE TRANSITION

A. General remarks

The CMR phenomenon occurs at a transition from itinerant to localized *d*-electron behavior. Therefore, two starting point can be used for the description of the electronic/structural properties at this crossover. One can begin with a description of the local properties of an isolated Mn ion in its crystalline surrounding and moves to a description of the system by introducing interaction between Mn ions. The other possibility is to ignore, at first, the individuality of the Mn ions and to treat the entire system as a medium characterized a common energy spectrum. The parent compound $LaMnO_3$ is an insulating antiferromagnet. As the doping level x is gradually increased from 0 to 0.05, the system does not exhibit a significant ferromagnetic ordering and metallic conductivity below the critical temperature. This means that holes introduced by doping and spatially extended over the sample are not able to mediate magnetic ordering. Therefore, a band theory of electronic states is not suitable starting point to describe itinerant to localized electronic behavior. A significant ferromagnetic ordering and sharp drop of resistivity occur at a higher doping level $0.2 \leqslant x \leqslant 0.4$. At this doping level the long-range periodicity in the crystal is destroyed and the conductivity has a rather pecolative nature. Therefore, there is reason to believe that a ''localized'' description of the electronic/structural properties at the crossover point is the appropriate starting place.

In the following, we describe a model of the ferromagnetic ordering among the Mn ions with the electron-phonon interaction explicitly included. Let us consider a single Mn^{3+} (or Mn^{4+}) ion in an octahedral oxygen environment. The $3d$ orbitals on the Mn site placed in such an octahedral coordination are subject to a partial lifting of the degeneracy into lower-lying t_{2g} states and higher-lying e_g states. The Mn^{3+} and Mn^{4+} ions have electronic configurations of $t_{2g}^3 e_g^1$ and t_{2g}^3, respectively. The local t_g electrons form the spin background for the e_g electrons. The e_g electrons play the role of conduction electrons, when electron vacancies are created in the e_g orbital states. In the following, we only consider the e_g states denoted by $d_{3z^2-r^2}$ and $d_{x^2-y^2}$. Our starting point is the magnetic cell with two Mn ions shown in

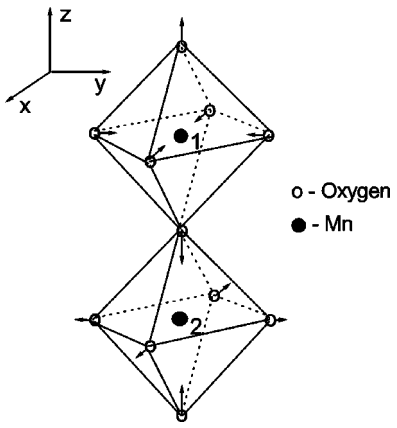

FIG. 1. Schematic structure of perovskites of manganite. The distortion of oxygen octahedrons of symmetry $Q_{3z^2-r^2}$ is shown.

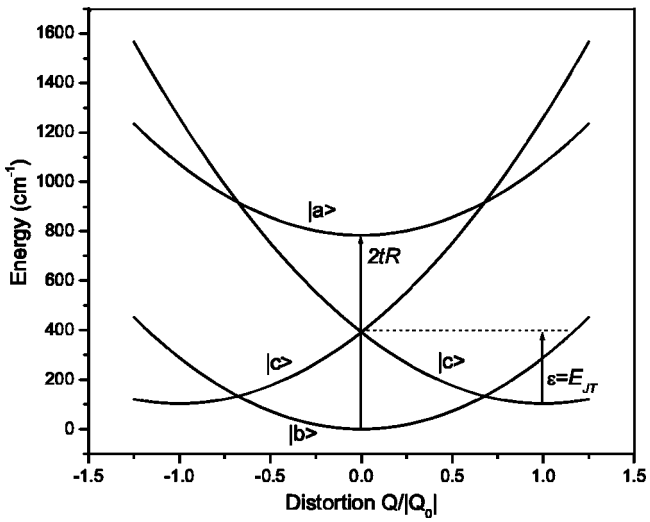

FIG. 2. The energy diagram of e_g states as a function of oxygen atom distortion from equilibrium positions. The states $|b\rangle = [d_{3z^2-r^2}(1) + d_{3z^2-r^2}(2)]/\sqrt{2}$ and $|c\rangle = d_{x^2-y^2}$, where 1 and 2 denote the position of Mn atoms in Fig. 1. The states $|a\rangle = [d_{3z^2-r^2}(1) - d_{3z^2-r^2}(2)]/\sqrt{2}$.

Fig. 1. The d orbitals of the neighboring Mn ions admix, bridged by the oxygen p orbitals.

The d-p transfer integral determines the width of the hybridized d bands. The group overlap integrals $\langle d_{3z^2-r^2}|p_{3z^2-r^2}\rangle$ and $\langle d_{x^2-y^2}|p_{x^2-y^2}\rangle$ between d functions and the respective oxygen molecular orbitals are equal to each other. Therefore, the e_g states are doubly degenerate. The Ca atom doping causes the transition of some Mn ions into the charge state Mn^{4+}. If we take into account the interaction between the second neighbors (Mn^{3+}- Mn^{4+}) then (at enough large doping level) the cubic symmetry around the Mn^{3+} ion is lowered and the degeneracy of e_g states is lifted. Consider the single Mn^{3+}-O^{2-}-Mn^{4+} chain shown in Fig. 1 along the z axis. The ionic radius of Mn^{3+} (Mn^{4+}) is 0.66 (0.60) Å whereas the ionic radius of O^{2-} is 1.32 Å. Therefore, the e_g states on the Mn^{3+} and Mn^{4+} ions interact by means of the oxygen bridging them. The $d_{3z^2-r^2}$ orbital has a nonvanishing overlap with the oxygen p_z orbital whereas the overlap of the $d_{x^2-y^2}$ orbital with the p orbitals is zero. Therefore, the $d_{3z^2-r^2}$ orbitals on the Mn neighboring sites form the bonding and antibonding states denoted by the $|b\rangle$ and $|a\rangle$, respectively. Similarly, as in Ref. 17, we introduce a transfer matrix element t between the d states; thus the states $|b\rangle$ and $|a\rangle$ are separated by the energy $2t$, as shown in Fig. 2. The $d_{x^2-y^2}$ states on both Mn sites interact significantly less than $d_{3z^2-r^2}$ states, and they form nonbonding states. We stress that the transfer integral t is between the second neighbors and it is remarkably smaller than the d-p transfer integral which mainly determines the width of the hybridized d bands. In our approximation, the width of all bands is taken as zero and it does not influence the magnetic properties. In the present model the energy gap between partly occupied $|b\rangle$ "band" and the nonbonding $d_{x^2-y^2}$ states is important. For the single Mn^{3+}-O^{2-}-Mn^{4+} chain the $|b\rangle$ state is occupied by one d electron. This electron hops spontaneously between the Mn sites, thus participating in the binding between two Mn ions. Since there is an enhanced density of the wave function on the bridging oxygen site, the e_g electron also partly resides on the oxygen. Due to the strong Coulomb correlation on Mn sites such hops are possible when the total spins of the t_{2g} electrons on both Mn sites are parallel. Thus the hopping of the e_g electrons along the Mn^{3+}-O^{2-}-Mn^{4+} chain causes a nonzero spontaneous magnetization. This hopping take place even at the zero temperature because in the bonding state the electron is equally shared between two sites. If the doping level is enough large, the e_g electrons can migrate among many Mn sites, ensuring the ferromagnetic ordering in the crystal. The excitation to the nonbonding $d_{x^2-y^2}$ states destroys the magnetization. Here we disregard the possible angles between neighboring Mn total spins, assuming a complete lining up of the spins. However, the effective magnetization can be lower than what is expected, not only due to the various angles between Mn ions, but also due to the formation of local domains with the opposite magnetization. In our description, we considered the bonding along the z axis. The equivalent description can be, say, along the x axis, taking the $d_{3x^2-r^2}$ and $d_{y^2-z^2}$ basis states. The basis states along the y axis are $d_{3y^2-r^2}$ and $d_{z^2-x^2}$.

It is well known that the octahedrally coordinated d^4 ions manifest the electron-phonon coupling which originates in the JT effect. Being a JT active ion, Mn^{3+} produces a static distortion of the surrounding oxygen atoms. This is due to the coupling of doubly degenerate electronic e_g states with tetragonal distortion (the $E-e$ problem[18]). The covalent binding of the e_g electron between Mn ions competes with the tetragonal distortion. In the upper part of Fig. 1 we show the $Q_{3z^2-r^2}$ component of the tetragonal distortion. This distortion has nonzero diagonal matrix elements within the space of $d_{3z^2-r^2}$ and $d_{x^2-y^2}$ bases.[18] The displacement of the bridging oxygen in the Mn^{3+}-O^{2-}-Mn^{4+} chain has the opposite direction with respect to both Mn ions. The states $|b\rangle$ and $|a\rangle$ are the linear combination of $d_{3z^2-r^2}$ functions on both Mn ions, i.e., $|b\rangle = [d_{3z^2-r^2}(1) + d_{3z^2-r^2}(2)]/\sqrt{2}$ and $|a\rangle = [d_{3z^2-r^2}(1) - d_{3z^2-r^2}(2)]/\sqrt{2}$. If we denote the displacement of bridging oxygen from the equilibrium by Q,

then, in the first approximation $\langle b|\partial V_{cryst}/\partial Q|b\rangle = \langle a|\partial V_{cryst}/\partial Q|a\rangle = 0$. For this reason the "adiabatic surface" of states $|b\rangle$ and $|a\rangle$ shown in Fig. 2 depends on Q^2 because it contains only the elastic energy. We assume that the interaction t is larger than the JT energy ε. We note that even if the Mn^{4+} ion is not JT active, the surrounding it oxygen octahedron is deformed due to the deformation in the vicinity of JT active Mn^{3+} neighbors. Contrary to the $d_{3z^2-r^2}$ functions, the $d_{x^2-y^2}$ function on the neighboring Mn ions are the nonbonding states (in the approximation of the second neighbor interaction) and their diagonal matrix element depends linearly on the displacement Q.[18] For this reason the nonbonding states have the energy minima at the displacement coordinates $\pm Q_0$ as it is shown in Fig. 2.

In this paper, we start from the consideration of the individual Mn^{3+}-O^{2-}-Mn^{4+} chain. We assume that these chains are distributed randomly in the crystal volume. The successive electron tunneling between various $Mn^{3+} \rightarrow Mn^{4+}$ pairs causes that crystal to exhibit a cooperative behavior: a ferromagnetic ordering at low temperatures. The thermal agitation of e_g electrons into the excited states $|c\rangle$ breaks the mutual ordering of individual pairs and transforms the crystal into the paramagnetic state.

B. Mathematical formulation

In the following description, we account only for the ground bonding state $|b\rangle$ and two excited nonbonding states $|c\rangle$. For simplicity, we consider only the $|c\rangle$ state with the minimum at positive displacement Q_0. The second $|c\rangle$ state is taken into account by the inclusion of the degeneracy factor $g=2$. The one-electron free energies f for the ground and exited states can be written as

$$f_{|b\rangle} = \frac{1}{2}kQ^2 - \mu H,$$

$$f_{|c\rangle} = tR - VQ + \frac{1}{2}kQ^2 - k_B T \ln g + \mu H, \tag{1}$$

where V is the electron-lattice coupling constant and k is the elastic force constant. The hopping integral t is multiplied by the Huang-Rhys factor R, μ is the magnetic moment, H is the external magnetic field, and k_B is the Boltzman constant. The displacement coordinate is $Q = 4/\sqrt{3}d$, where d is the change of the equilibrium Mn-O bond length. The Zeeman energy in the excited state is taken with the opposite sign with respect to the ground state because the electron in this state is bound only to one Mn ion (nonbonding state). When the electron occupies one of the $|c\rangle$ state, there is no correlation between the background spins on neighboring Mn ions. They can be parallel or antiparallel, and this situation corresponds to the paramagnetic phase. Since the net spontaneous magnetic moment of the crystal in the paramagnetic phase is equal to zero, we assume that the background spins have opposite direction in the Mn^{3+}-O^{2-}-Mn^{4+} chain.

Now we shall define the e_g electron distribution function which depends on the model parameters and the temperature. At $T=0$ K, the electron occupies the ground state $|b\rangle$ and the average bridging oxygen displacement is zero due to the fast tunneling between two Mn sites. The electron is equally distributed between two Mn ions. For the optimal concentration of holes the resistivity of the crystal is metal-like. With the increase of temperature the ground state admixes the excited states $|c\rangle$. At some high enough temperature the admixture is so large that the e_g electron spends time mainly around one of the Mn ions, i.e., it is mainly on the $d_{x^2-y^2}$ orbital and the oxygen displacement shifts towards $Q=Q_0$. For intermediate temperatures the displacement is $0<Q<Q_0$. We define the distribution function n as $n=Q/Q_0$ and $n \in [0,1]$. At the deformation Q_0 the energy gain is $\varepsilon \equiv E_{JT} = V^2/2k = kQ_0^2/2$. Using our notation the free energies can be expressed as

$$f_{|b\rangle} = \varepsilon n^2 - \mu H,$$
$$f_{|c\rangle} = tR - 2\varepsilon n + \varepsilon n^2 - k_B T \ln g + \mu H. \tag{2}$$

The free energy F of the system for the temperature T is written as

$$F = f_{|b\rangle} - k_B T \ln\left[1 + \exp\left(\frac{-(f_{|c\rangle} - f_{|b\rangle})}{k_B T}\right)\right]$$
$$= \varepsilon n^2 - \mu H - k_B T \ln\left[1 + g \exp\left(-\frac{tR - 2\varepsilon n + 2\mu H}{k_B T}\right)\right]. \tag{3}$$

In the thermal equilibrium, the distribution n is determined by a minimization of the free energy F with respect to n, which gives

$$n = \frac{g \exp\left(-\frac{tR - 2\varepsilon n + 2\mu H}{k_B T}\right)}{1 + g \exp\left(-\frac{tR - 2\varepsilon n + 2\mu H}{k_B T}\right)}. \tag{4}$$

The distribution n is the probability of the paramagnetic phase. The distribution

$$1 - n = \frac{1}{1 + g \exp\left(-\frac{tR - 2\varepsilon n + 2\mu H}{k_B T}\right)} \tag{5}$$

is the probability of the ferromagnetic phase. At the critical temperature T_C the ferromagnetic and paramagnetic fractions are at equilibrium, i.e., $n = 1-n = 1/2$. Using this condition it follows from Eqs. (4) and (5) that

$$T_C = \frac{tR - \varepsilon + 2\mu H}{k_B \ln g}. \tag{6}$$

The ferromagnetic phase excess Δn is determined as $\Delta n = (1-n) - n = 1 - 2n$. Using Eqs. (4) and (5) one obtains

$$\frac{tR - \varepsilon + 2\mu H + \varepsilon \Delta n}{k_B T} - \ln g = \ln\left(\frac{1 + \Delta n}{1 - \Delta n}\right). \tag{7}$$

At the critical temperature (when $\Delta n \to 0$) the last equation gives

$$\frac{\varepsilon}{k_B T_C} = \lim_{\Delta n \to 0} \frac{1}{\Delta n} \ln\left(\frac{1+\Delta n}{1-\Delta n}\right) \to 2. \tag{8}$$

By inserting $\varepsilon = 2kT_C$ into the expression for T_C, one finds

$$tR = k_B T_C (2 + \ln g) - 2\mu H. \tag{9}$$

Thus the model parameters ε and tR can be approximately determined from the experimental knowledge of the critical temperature T_C. Assuming $H=0$, one finds the ratio $tR/k_B T_C = 2 + \ln g \approx 2.7$. The value of similar ratio for superconductors is in the range 2–7.[19]

It is interesting to know the functional dependence of Δn on T near the phase transition point. To this purpose, we insert the series expansion

$$\ln\left(\frac{1+\Delta n}{1-\Delta n}\right) = 2\left(\Delta n + \frac{\Delta n^3}{3} + \cdots\right), \quad |\Delta n| < 1 \tag{10}$$

into Eq. (7). After some rearrangements one obtains the expressions

$$\left(\frac{T_C}{T} - 1\right)(\ln g + 2\Delta n) = \frac{2}{3}\Delta n^3,$$

$$\Delta n \approx \left[\frac{3}{2} \ln g \left(\frac{T_C}{T} - 1\right)\right]^{1/3}, \tag{11}$$

where $2\Delta n$ was neglected in the sum $\ln g + 2\Delta n$. Equation (11) describes the temperature dependence of the magnetization $M = (1-2n)\mu = \Delta n \mu$ just below T_C. This result is in good agreement with the observations of the spontaneous magnetization. In the context of Landau's theory of the second-order phase transition[20] the Δn plays the role of the order parameter. Using $n = (1-\Delta n)/2$ in Eq. (3) and then taking the series expansion over Δn one finds that, in the vicinity of the critical temperature, the free energy depends on the even powers of Δn.

The free energy [Eq. (3)] can be rewritten in the conventional form $F = U - TS$ that is more convenient for applications. Using Eq. (3) one finds the entropy S

$$S = -\left(\frac{\partial F}{\partial T}\right)_V = -k_B[-n \ln g + n \ln n + (1-n)\ln(1-n)]. \tag{12}$$

Using Eq. (3) again and the expression for the entropy, one finds the internal energy of system U:

$$U = -\varepsilon n^2 + ntR - \mu(1-2n)H. \tag{13}$$

Taking into account the explicit expression for the internal energy U one can calculate the electronic contribution to the heat capacity C_V,

$$C_V = \frac{\partial U}{\partial T} = (-2\varepsilon n + tR + 2\mu H)\frac{dn}{dT}, \tag{14}$$

where

$$\frac{dn}{dT} = \frac{n(1-n)k_B \ln^2[n/g(1-n)]}{2\varepsilon n(1-n)\ln[n/g(1-n)] + (tR - 2\varepsilon n + 2\mu H)}. \tag{15}$$

The free energy F as given by Eq. (3) can be transformed to the form that is typical for the simple Ising model of ferromagnetism.[20] The transformed free energy F_I is of the form

$$F_I = -\varepsilon n^2 - MH + (tR - k_B T \ln g)n + k_B T[n \ln n + (1-n)\ln(1-n)], \tag{16}$$

where the first term containing $\varepsilon \equiv ZJ(\mathbf{S}_1\mathbf{S}_2)$ ($Z=6$ is the coordination number for the cubic lattice, J is the exchange integral, and $\mathbf{S}$ is the spin) describes the exchange interaction between neighboring spins, the second is the Zeeman energy, the third corresponds to the free energy of excited state, and the last gives the contribution from the mixing entropy. F and F_I are equivalent in that they have the identical extremal points, i.e., they lead to the distribution function n, as it is given by Eqs. (4) and (5).

C. Isotope effect

A series of observations[5–8] reported on a large mass dependent shift of the critical phase transition temperature. Zhao *et al.*[5] found a giant oxygen-isotope shift of the transition temperature of $La_{0.80}Ca_{0.20}MnO_3$. By replacing ^{16}O with ^{18}O a decrease in $T_C \sim 20$ K was observed, an unambiguous evidence of electron-lattice coupling. The oxygen isotope coefficient is defined as

$$\alpha = -d \ln T_C / d \ln M_O = -\frac{M}{T_C}\frac{dT_C}{dM_O}, \tag{17}$$

where M_O is the oxygen isotope mass. The critical temperature [Eq. (6)] depends on the oxygen mass by means of the Huang-Rhys factor $R = \exp(-\varepsilon/2\hbar\omega)$. This factor is the overlap of the ground-state oscillator functions centered at the average position of oxygen and in the distorted position. Taking the derivative of T_C over M_O, one obtains

$$\alpha = \frac{1}{2\ln g}\left(\frac{t}{k_B T_C}\right)\left(\frac{\varepsilon}{2\hbar\omega}\right)\exp\left(\frac{-\varepsilon}{2\hbar\omega}\right) = \frac{1}{2}\frac{tR}{tR - \varepsilon + 2\mu H}\left(\frac{\varepsilon}{2\hbar\omega}\right). \tag{18}$$

In an estimation of the isotope coefficient we use the right hand of the last equation because we treat the product of t and R as one adjustable parameter. Taking $H=0$ and using Eqs. (8) and (9) one obtains, from Eq. (18),

$$\alpha = \left(\frac{1}{\ln 2} + \frac{1}{2}\right)\left(\frac{\varepsilon}{2\hbar\omega}\right). \tag{19}$$

The last equation shows that α depends only on the JT energy and the vibration frequency of oxygen in the Mn-O bond. In Ref. 5 the relation $T_C \propto W \exp(-\gamma\varepsilon/\hbar\omega)$ was postulated, where W is the bare conduction bandwidth and the

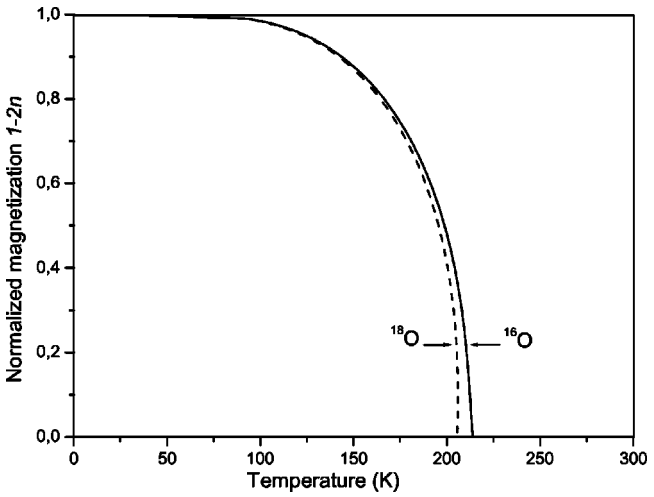

FIG. 3. The normalized magnetization $M/M_0=1-2n$ calculated for the model parameters $\varepsilon=289\ \mathrm{cm}^{-1}$ and $tR=392\ \mathrm{cm}^{-1}$. The shift of T_C due to isotope substitution $^{16}\mathrm{O}\rightarrow{}^{18}\mathrm{O}$ is shown.

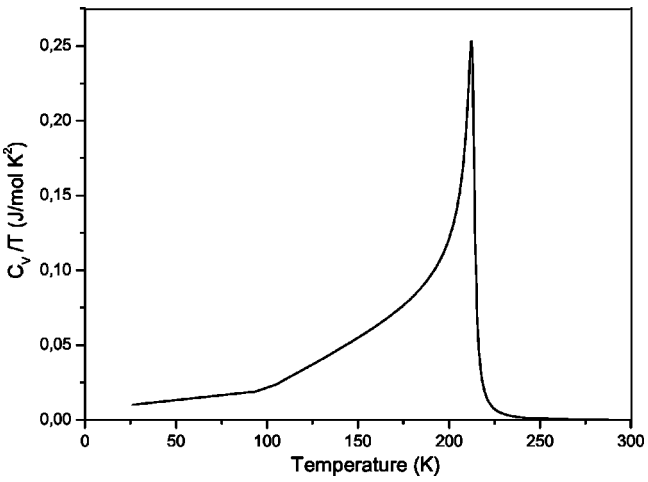

FIG. 4. The peak of the electronic specific heat capacity C_V (divided by temperature) at the critical temperature.

dimensionless parameter $0<\gamma\leqslant 1$. Then the isotope coefficient is $\alpha=\gamma\varepsilon/2\hbar\omega$. Equation (19) obtained on the basis of the present model is indeed of the same form as that in Ref. 5. However, in contradiction to Ref. 5, our coefficient $\gamma=\ln^{-1}2+0.5=1.94$ exceeds the range given in Ref. 5. The isotope coefficient vanish when the JT energy $\varepsilon\rightarrow 0$. The small value of α was observed in some superconductors.[19]

III. RESULTS AND DISCUSSION

The important result obtained in Sec. II is the distribution function n of the e_g electrons. This function enters into various formulas for the calculation of physical properties. If the saturated magnetization at $T=0$ K is M_0, then the spontaneous magnetization at the temperature T is given as $M/M_0=1-2n$. The magnetization is equal to zero for the $n=1/2$, which corresponds, by definition, to the critical temperature. In Fig. 3 we plot the $1-2n$ function. The parameters $\varepsilon=289\ \mathrm{cm}^{-1}$ and $tR=392\ \mathrm{cm}^{-1}$ were adjusted so as to reproduce the critical temperature ≈ 210 K for the $La_{0.8}Ca_{0.2}MnO_3$ crystal.[5] At the critical temperature the slope of $1-2n$ is a sensitive function of ε and tR. To determine these parameters we take into account relations (8) and (9). It is seen that the $1-2n$ curve reproduces well the steep jump of the magnetization when the critical temperature T_C is approached.

Measurements of the specific heat[13–16] is widely used for the investigation of the phase transitions. The specific heat capacity, as given by Eq. (14), depends not only on the distribution n but also on its temperature derivative $\partial n/\partial T$ as given by Eq. (15). This is the reason why the peak of the specific heat shown in Fig. 4 does not coincide with the T_C (in the present case it is shifted to lower temperatures by about 1.5 K). The calculation of the electronic contribution to the specific heat is a very strong test of the distribution function. Experimentally, the contribution given by Eq. (14) is observed together with the lattice vibration contribution,[13] which is usually well accounted by the Debye theory. As established by x-ray diffraction,[10] the change of electronic configuration is associated with the small change of the lattice volume. However, this volume change makes a negligible contribution to the lattice vibrations because the vibrational specific heat can be well approximated by only one value of the Debye temperature. In the opposite case, the lattice contribution before and above the critical point would be two different curves because of the volume-dependent frequency change. The experimental specific heat of the $La_{0.8}Ca_{0.2}MnO_3$ crystal shown in Fig. 1 of Ref. 1 does not exhibit any significant volume change at T_C. The peak of the specific heat at T_C calculated in the present work reproduces well the experimental one.[13,16]

The estimation of the isotope coefficient α requires the knowledge of the oxygen vibration frequency in the Mn-O bond. We estimate the vibrational frequency using the Harrison semiempirical theory[21] for the bond energy. The equilibrium distance d_0 at zero temperature is determined from the minimum of the Helmholtz free energy F_{bond}, for the Mn-O bond,

$$F_{bond}=\varepsilon_b+\hbar\omega/2, \tag{20}$$

where ε_b is the bond energy and $\hbar\omega/2$ is vibration energy at the temperature 0 K. The t_{2g} orbital of the d electrons and the p_x, p_y, p_z orbitals of oxygen (denoted as x, y, z) contribute significantly to the Mn-O bonds in such crystals as $CaMnO_3$ and $LaMnO_3$. In the nearest-neighbor approximation they form π-type bonds, i.e., d_{xy}-y and d_{xz}-z bonds along X axes, d_{xy}-x and d_{yz}-z bonds along Y axes, and d_{yz}-y and d_{xz}-x bonds along Z axes. For the π bond, the bond energy ε_b is given by[22]

$$\varepsilon_b=\frac{(\varepsilon_d+\varepsilon_p)}{2}-q\sqrt{V_2^2+\left(\frac{\varepsilon_d-\varepsilon_p}{2}\right)^2}+\frac{2qV_2^2}{k|\varepsilon_d+\varepsilon_p|}, \tag{21}$$

where $V_2=17.72/d_0^{7/2}$ is the Coulomb interaction matrix element between d-p electronic functions, $q=2$ is the number of electrons per bond, and ε_d and ε_p are the free atomic electron eigenvalues for the d electrons of Mn and p elec-

trons of oxygen. Taking into account that $\omega = \sqrt{(\partial^2 \varepsilon_b / \partial d^2)/\mu}$, the condition of minimum for the F_{bond} is

$$\frac{\partial \varepsilon_b}{\partial d} + \frac{\hbar}{4\sqrt{\mu_r}} \frac{\dfrac{\partial^3 \varepsilon_b}{\partial d^3}}{\sqrt{\dfrac{\partial^2 \varepsilon_b}{\partial d^2}}} = 0, \tag{22}$$

where μ_r is the reduced mass for the bond. The first term in Eq. (22) determines the equilibrium distance from the minimum of the Coulomb interaction energy only. It does not depend on the isotope substitution. The second term in Eq. (22) depends on the isotope mass. The third derivative of ε_b in the second term accounts for the anharmonicity of the interatomic Coulomb interaction. It is seen from Eq. (22) that the interatomic distance depends on the isotope mass. It also follows that the harmonic force constant, which is calculated at the equilibrium distance, depends indirectly on the isotope mass. Equation (21) contains one adjustable parameter, k, which is determined from the condition that the calculated bond length of the Mn-^{16}O is equal to the experimental value 1.97 Å. Thus we obtained $k=0.24$, and with this value the Mn-^{18}O bond length can be estimated.

We found that when ^{16}O is replaced by ^{18}O the Mn-O bond length is decreased by 0.0005 Å, i.e., by $\approx 0.025\%$. Such a replacement increases the harmonic stretching force constant $k_h = \partial^2 \varepsilon_b / \partial d^2$ from 8.355 to 8.387 eV/Å^2 (i.e., by $\approx 0.38\%$) The stretching frequency ω_{strech} of the Mn-O pair decreases from 426 to 408 cm^{-1} (i.e. by $\approx -4.2\%$) mainly due to the increase of the isotope mass. Recently Irwin *et al.*[7] observed the Raman spectra of a $La_{0.65}Ca_{0.35}MnO_3$ crystal. They observed the high-energy mode at 435 cm^{-1} which was shift to 415 cm^{-1} (i.e., decreased by -4.6%) upon substitution of ^{16}O by ^{18}O. The agreement of the calculated oxygen frequency shift with the experimental one indicates that parameters used in the calculation are reliable. Taking the stretching frequency of the ^{16}O $\hbar\omega = 426$ cm^{-1} and using the value $tR = 392$ cm^{-1}, $\varepsilon = 289$ cm^{-1} we obtain $\alpha = 0.65$. The value determined directly from measurement of magnetization is $\alpha \sim 0.85$.[5]

The other test of the model is the effect of the CMR. The calculation of the resistivity requires accounts for the electron scattering and percolation processes, and is beyond the scope of these calculations. However, the resistivity is inversely proportional to the distribution function. Below the critical point the number of carries is approximately proportional to $1/(1-n)$, whereas above the critical point to $1/n$. Figure 5 shows the resistivity calculated in this way for magnetic fields equal to zero and to 1 T. In reality, the proportionality between resistance and $1/n$ $[1/(1-n)]$ includes a mobility factor. Drawing the resistivity in Fig. 5, we assumed that the mobility weakly changes with temperature near the phase transition point. It is seen from Eq. (6) that Zeeman energy changes the balance between tR and ε and, thus, affects the critical temperature. When the external magnetic field is switched off, the critical temperature depends on the

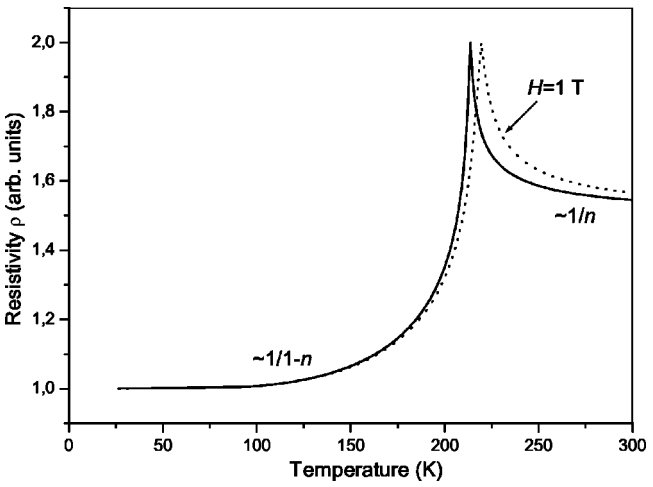

FIG. 5. The resistivity $\rho \propto 1/1-n$ below the critical point and $\rho \propto 1/n$ above the critical point. The shift of the critical point is due to the external magnetic field of 1 T.

energy difference $tR-\varepsilon$. Because in the states $|b\rangle$ and $|c\rangle$ the spin of e_g electrons has a different orientation, the magnetic field increases the energy gap between states $|b\rangle$ and $|c\rangle$ and, thus, according to Eq. (6) this leads to the increase of the critical temperature. The critical temperature is increased by 6 K because the external field that is added to the Weiss ''molecular'' field enhances ferromagnetic ordering against the destructive action of temperature. This action of the magnetic field explains the CMR effect. Due to the presence of an energy gap between the ground and excited states and due to the spin ordering on Mn sites, the conductivity is large below the critical temperature. These two facts prevent the scattering of the e_g electrons into the excited state $|c\rangle$, and the electrons freely hop among the Mn sites, being in the ground state $|b\rangle$. The crystal will exhibit the metal-like conductivity in an electric field. The electrons hopping along the Mn-O-Mn bonds lead not only to spontaneous fluctuations of the charge states but also to intrinsic distortions associated with the charge state—the polaron.

Near and above the critical point the vibrations affect more effectively the scattering and this results in the large resistivity. The abrupt change of the partition function is not only responsible for the CMR. It also influences the large entropy change of the phase transition, the lattice volume change (not associated with the breathing mode distortion), the sharp thermal expansion coefficient increase at T_C, and the Debye-Waller factor change. We reserve the consideration of these effect to the other paper.

In conclusion, we described the two-parameter model of the FP phase transition. The parameters characterize the electron-phonon coupling and the effect of covalent binding. The partition function n can describe, as a function of T, the gradual or abrupt transition between the ferromagnetic and paramagnetic phases depending on the model parameters. The essential condition for the abrupt transition is that the ground and excited electronic states have the minima at different displacement coordinates Q. If the minima are at the same displacement coordinate ($\varepsilon = 0$), the partition function

n of Eq. (4) for the FP phase transition is the Boltzman like and the transition is gradual. Not only is the abrupt nature of the phase transition reproduced, but the sharp peak in the electronic specific heat capacity is also reproduced. Finally, we note the close analogy between free energy following from the present model and that one used in the simple version of the Ising model [Eq. (16)], provided we substitute ε by $ZJ(\mathbf{S}_1\mathbf{S}_2)$; also see Ref. 22.

ACKNOWLEDGEMENT

We are grateful for valuable discussions with Professor A. Sienkiewicz.

*Email address: biern@ifpan.edu.pl

[1] C. Zener, Phys. Rev. **82**, 403 (1951).
[2] Yu. A. Izyumov and Yu N. Skryabin, Usp. Fiz. Nauk. **171**, 121 (2001) [Phys. Usp. **44**, 109 (2001)].
[3] A. Chattopadhyay, A. J. Millis, and S. Das Sarma, cond-mat/9908305 (unpublished).
[4] Guo-meng Zhao, Phys. Rev. B **62**, 11 639 (2000).
[5] G. Zhao, K. Conder, H. Keller, and M. A. Müller, Nature (London) **381**, 676 (1996).
[6] I. Isaac and J. P. Franck, Phys. Rev. B **57**, R5602 (1998).
[7] J. C. Irwin, J. Chrzanowski, and J. P. Franck, Phys. Rev. B **59**, 9362 (1999).
[8] V. Chechersky, A. Nath, I. Isaac, J. P. Franck, K. Ghosh, and R. L. Greene, Phys. Rev. B **60**, 3005 (1999).
[9] P. Dai, J. Zhang, H. A. Mook, S.-H. Liou, P. A. Dowben, and E. W. Plummer, Phys. Rev. B **54**, R3694 (1996).
[10] P. G. Radaelli, D. E. Cox, M. Marezio, S.-W. Cheong, P. E. Schiffer, and A. P. Ramirez, Phys. Rev. Lett. **75**, 4488 (1995).
[11] K. Khazeni, Y. X. Jia, Li Lu, V. H. Crespi, M. L. Cohen, and A. Zettl, Phys. Rev. Lett. **76**, 295 (1996).
[12] Y. S. Wang, A. K. Heilman, B. Lorenz, Y. Y. Xue, C. W. Chu, J. P. Franck, and W. M. Chen, Phys. Rev. B **60**, R14 998 (1999).
[13] J. Tanaka and T. Mitsuhashni, J. Phys. Soc. Jpn. **53**, 24 (1984).
[14] A. P. Ramirez, P. Schiffer, S.-W. Cheong, C. H. Chen, W. Bao, T. T. M. Palstra, P. L. Gammel, D. J. Bishop, and B. Zegarski, Phys. Rev. Lett. **76**, 3188 (1996).
[15] J. M. D. Coey, M. Viret, L. Ranno, and K. Ounadjela, Phys. Rev. Lett. **75**, 3910 (1996).
[16] L. Ghivelder, I. Abrego Castillo, N. McN. Alford, G. J. Tomka, P. C. Riedi, J. MacManus-Driscoll, A. K. M. Akther Hossain, and L. F. Cohen, J. Magn. Magn. Mater. **189**, 274 (1998).
[17] P. G. de Gennes, Phys. Rev. **118**, 141 (1960).
[18] M. D. Sturge, in *Solid State Physics*, edited by D. T. F. Seitz and H. Eherennreich (Academic Press, New York, 1967), Vol. 20, p. 99.
[19] N. Tsuda, K. Nasu, A. Fujimori, and K. Siratori, *Electronic Conduction in Oxides*, second revised edition (Springer-Verlag, Berlin, 2001).
[20] C. Daniel and Ph. D. Mattis, *The Theory of Magnetism* (Harper and Row, New York, 1965), Chap. 8.
[21] W. A. Harrison, *Electronic Structure and the Properties of Solids* (Freeman, New York, 1980), Chaps. 2 and 19.
[22] R. A. Bari and J. Sivardiere, Phys. Rev. B **5**, 4466 (1972).